



# Extreme lowering of deglacial seawater radiocarbon recorded by both epifaunal and infaunal benthic foraminifera

Patrick A. Rafter<sup>1</sup>, Juan-Carlos Herguera<sup>2</sup>, John R. Southon<sup>1</sup>

<sup>1</sup>Department of Earth System Science, University of California, Irvine, CA, USA

5 <sup>2</sup> Centro de Investigación Científica y Educación Superior de Ensenada, Mexico

Correspondence to: Patrick A. Rafter ([prafter@uci.edu](mailto:prafter@uci.edu))

**Abstract.** For over a decade, oceanographers have debated the interpretation and reliability of sediment microfossil records indicating extremely low seawater radiocarbon ( $^{14}\text{C}$ ) during the last deglaciation—observations that suggest a major disruption in marine carbon cycling coincident with rising atmospheric  $\text{CO}_2$  concentrations. Possible flaws in these records include poor age model controls, utilization of mixed, infaunal foraminifera species, and bioturbation. We have addressed these concerns using a glacial-interglacial record of epifaunal benthic foraminifera  $^{14}\text{C}$  on an ideal sedimentary age model (wood calibrated to atmosphere  $^{14}\text{C}$ ). Our results affirm—with important caveats—the fidelity of these microfossil archives and confirm previous observations of highly depleted seawater  $^{14}\text{C}$  at intermediate depths in the deglacial northeast Pacific.

## 1 Introduction

15 Given modern carbon cycle perturbations (Keeling, 1960), it is critical to understand the drivers of natural atmospheric carbon dioxide ( $\text{CO}_2$ ) variability. A prime example of this ‘natural’ atmospheric  $\text{CO}_2$  variability is the increase that occurs at the end of each late-Pleistocene ice age (Figure 1) (Petit et al., 1999). The ocean’s ability to store and release  $\text{CO}_2$  makes it a likely driver of past changes in this important greenhouse gas (Broecker, 1982).

20 A valuable tool in the effort to characterize the marine carbon cycle over the most recent of these intervals is the  $^{14}\text{C}$  content of benthic and planktic foraminifera tests (Broecker et al., 1988), which are assumed to reflect the  $^{14}\text{C}$  content of dissolved inorganic carbon (DIC) in the waters in which they grew. This tracer provides a geochemical “clock” with a predictable decay but  $^{14}\text{C}$  is also affected by a variety of other processes, including the time since the water mass exchanged  $\text{CO}_2$  with the atmosphere, the degree of this exchange, variations in the atmospheric concentration of  $^{14}\text{C}$  at the time of exchange  
25 (Figure 1), as well as the contribution of  $^{14}\text{C}$ -depleted carbon via mixing and / or other carbon sources (e.g., seafloor volcanism (Ronge et al., 2016)).

We can relate seawater  $^{14}\text{C}$  content to modern ocean conditions by using delta notation or  $\Delta^{14}\text{C}$  (Figure 1), which corrects for  $^{14}\text{C}$  decay:



$$\Delta^{14}\text{C} = e^{(-^{14}\text{C age}/8033)} / e^{(-\text{Calendar Age}/8267)} - 1 \quad (1)$$

(Equation (1) is multiplied by 1000 to give units of per mil [‰]. The  $^{14}\text{C}$  age Calendar Age is given in years before 1950 or “before present” (BP).)

The available benthic foraminifera  $\Delta^{14}\text{C}$  records paint a complicated picture of glacial to interglacial seawater  $^{14}\text{C}$  content. For example, a record of benthic foraminifera  $\Delta^{14}\text{C}$  from the intermediate depth subtropical eastern North Pacific (Lindsay et al., 2015; Marchitto et al., 2007) shows  $\Delta^{14}\text{C}$  depleted relative to the atmosphere by  $>500\text{‰}$  during the deglaciation (from  $\approx 19\text{-to-}11,000$  years BP; see Figure 1). Later work showed benthic foraminifera with similar or even lower  $\Delta^{14}\text{C}$  values during the deglaciation in other parts of the intermediate depth ocean ( $\approx 500\text{-}1000$  m), such as the 617 m deep Eastern Equatorial Pacific (Stott et al., 2009) and the 596-820 m deep Arabian Sea (Bryan et al., 2010). Given that the lowest observed modern intermediate-depth seawater  $\Delta^{14}\text{C}$  is about  $-300\text{‰}$  (or only  $\approx 300\text{‰}$  lower than the atmosphere) (Key et al., 2004), the low benthic foraminifera  $\Delta^{14}\text{C}$  / old  $^{14}\text{C}$  ages suggest much lower  $\Delta^{14}\text{C}$  and older seawater DIC  $^{14}\text{C}$  ages during the deglaciation.

A leading explanation of these low intermediate depth  $\Delta^{14}\text{C}$  values involves the storage of carbon in an isolated deep-sea reservoir during the glacial period followed by the rapid flushing of this low  $\Delta^{14}\text{C}$  / old  $^{14}\text{C}$  aged carbon through the intermediate-depth ocean during the deglaciation (Marchitto et al., 2007; Figure 1)—a deep-sea carbon flush that also explains the observed elevation of atmospheric  $\text{CO}_2$  concentrations and lowering of atmospheric  $\text{CO}_2$   $^{14}\text{C}$  content (Broecker & Barker, 2007). This interpretation is qualitatively supported by observations of lower deep-sea dissolved oxygen concentrations before the deglaciation (Jaccard et al., 2016; Jaccard and Galbraith, 2011).

The ocean carbon flushing hypothesis predicts that deep-sea  $\Delta^{14}\text{C}$  during the glacial period will be equal to or lower than the extreme  $\Delta^{14}\text{C}$  lowering of the intermediate-depth  $\Delta^{14}\text{C}$  during the deglaciation (Figure 1). However, while lower  $\Delta^{14}\text{C}$  is observed in some deep-sea waters during the glacial period (Sikes et al., 2000; Skinner et al., 2010; Keigwin and Lehman, 2015) and intermediate-depth waters during the deglaciation (Burke and Robinson, 2012), it is not clear how these low  $\Delta^{14}\text{C}$  signals are able to propagate to the lower latitudes (Hain et al., 2011). Additionally, the lower  $\Delta^{14}\text{C}$  in Figure 1 is not observed at all intermediate depth sites during the deglaciation (De Pol-Holz et al., 2010; Rose et al., 2010). Furthermore, the extreme  $\Delta^{14}\text{C}$  lowering observed in intermediate-depth benthic foraminifera during the deglaciation does not appear to be quantitatively consistent with an isolated deep-sea reservoir (Hain et al., 2011).

The inconsistency of the available  $\Delta^{14}\text{C}$  records is compounded by assumptions about the reliability of the foraminifera



archive as a recorder of seawater DIC  $^{14}\text{C}$ . For example, an important assumption when using planktic foraminifera is that they do not migrate vertically and are therefore recording seawater conditions at a static depth (e.g., (Field, 2004)). The use of benthic foraminifera seemingly circumvents this problem, but the abundance of benthic foraminifera that live at the sediment-water interface (“epifaunal”) is low relative to benthic species that abide within the sediment (“infaunal”). Rather than recording seawater  $^{14}\text{C}$  content directly, the infaunal species provide a record of sediment pore water carbon chemistry, which may or may not reflect bottom water conditions.

A further complication to published benthic foraminifera  $\Delta^{14}\text{C}$  observations is that both the epifaunal and infaunal species are typically rare in sediments, leading to the use of mixed benthic species which in at least some cases have been shown to give anomalously low  $\Delta^{14}\text{C}$  values / old  $^{14}\text{C}$  ages (Magana et al., 2010): in fact, we are unaware of any glacial-interglacial records of mono-species epifaunal foraminifera  $^{14}\text{C}$  content. (One study used mixed planispiral species, whose morphology predicts an epifaunal habitat (Galbraith et al., 2007).) An additional influence on benthic foraminifera  $\Delta^{14}\text{C}$  is bioturbation (Keigwin and Guilderson, 2009), which is infrequently taken into consideration, even though it can dramatically affect the observed  $^{14}\text{C}$  age (Costa et al., 2018). The doubts raised by the above complications are amplified by converting the benthic foraminifera  $^{14}\text{C}$  age to  $\Delta^{14}\text{C}$ , which requires the user to assign a calendar age to the sediment. For our understanding of past and future carbon cycling processes, it is essential that we thoroughly explore these influences and build confidence in these sediment proxy records.

Here, we provide a wide-ranging test of the fidelity of the benthic foraminifera  $\Delta^{14}\text{C}$  proxy using  $^{14}\text{C}$  measurement of benthic foraminifera species from two sediment cores near the mouth of the Gulf of California (white diamond in Figure 2). These sediment cores are unusual in that both epifaunal and infaunal benthic foraminifera microfossils are plentiful and allow us a unique opportunity to test the fidelity of the benthic foraminifera  $\Delta^{14}\text{C}$  proxy. The foraminiferal abundance were quantified to account for bioturbation and the age model is calibrated to the well-constrained atmospheric  $^{14}\text{C}$  record (Reimer et al., 2013) via wood found alongside the foraminifera. These cores (from hereon, the ‘Gulf’ sites) allow us to present glacial-interglacial  $^{14}\text{C}$  measurements produced from 4 benthic foraminifera, including the preferred epifaunal species *Planulina ariminensis* (Keigwin, 2002). The Gulf core sites are bathed in the subsurface, northward flowing Mexican Coastal Current (MCC in Figure 2), which are the source of the California Undercurrent (Gómez-Valdivia et al., 2015)—waters that also bathe the well known sites on the Pacific margin of Baja California shown in Figure 1 (from hereon, the ‘California Undercurrent’ sites). This shared seawater source gives the expectation of similar  $\Delta^{14}\text{C}$  signal at both sedimentary locations—an expectation that we exploit to examine the potential for diagenetic alteration of the benthic foraminifera  $\Delta^{14}\text{C}$  observations relative to sedimentation rates, which are significantly lower at the Gulf sites ( $\approx 2$  to  $5\text{ cm kyr}^{-1}$ ; our study) relative to the Undercurrent sites ( $>25\text{ cm kyr}^{-1}$ ; (Lindsay et al., 2015; Marchitto et al., 2007)). These and other hydrological, geochemical, and diagenetic influences on benthic foraminifera  $\Delta^{14}\text{C}$  are examined below with the goal of answering an



important question: are these benthic foraminifera  $\Delta^{14}\text{C}$  records recording an extreme lowering of seawater  $\Delta^{14}\text{C}$  during the deglaciation?

## 2 Materials and Methods

- 5 Sediment from Gulf of California sites LPAZ-21P (22.9°N, 109.5°W; 625 m) and ET97-7T (22.9°N, 109.5°W; 640 m) (white diamond in Figure 2) was washed using de-ionized water in a 63- $\mu\text{m}$  sieve. Foraminifera abundance estimates of *Planulina ariminensis* (benthic; epifaunal species), *Uvigerina peregrina* (benthic; shallow infaunal species), *Trifarina bradyi* (benthic; deep infaunal species), mixed *Bolivina* (benthic; deep infaunal species), and *Globogerina bulloides* (planktic species) were made after quantitatively dividing each sample using a Green Geological aluminum microsplitter. These
- 10 estimates were made for all samples from core LPAZ-21P and select samples from core ET97-7T. Preliminary work measured the  $^{14}\text{C}$  age of mixed benthic species from the ET97-7T core site and although the species abundance was not quantified, they primarily included *Planulina* spp., *Uvigerina* spp., and *Trifarina* spp.

### 2.1 Radiocarbon measurements

- 15 Monospecies foraminifera and wood were selected for  $^{14}\text{C}$  analysis from the  $>250\text{ }\mu\text{m}$  fraction from both Gulf sediment cores. Each foraminifera sample was sonicated in methanol ( $\approx 1$  minute) to release detrital carbonates trapped within open microfossil chambers. At least 10% of each sample was dissolved using HCl to remove secondary calcite (precipitated post-deposition), though in-house tests with and without this pretreatment yielded identical results for these core sites. Wood fragments from the  $>250\text{ }\mu\text{m}$  fraction were prepared using standard acid-base-acid
- 20 treatments.

- Samples were graphitized following (Santos et al., 2007) and analyzed at the Keck Carbon Cycle Accelerator Mass Spectrometry (KCCAMS) laboratory at University of California, Irvine (Southon et al., 2004). We report radiocarbon as  $\Delta^{14}\text{C}$  in units of per mil [‰] (see equation (1) above), which is corrected for decay based on its age normalized to
- 25 1950, according to convention (Stuiver and Polach, 1977). Analysis of a sedimentary standard (FIRI-C) alongside measurements indicates a combined sample preparation and measurement  $^{14}\text{C}$  age error ranging from  $\pm 50$  years for a full size sample ( $\approx 0.7\text{ mg}$ ) to  $\pm 500$  years for very small samples ( $< 0.1\text{ mg}$ ). Because of the similar location of the sites near the mouth of the Gulf of California, we combined the  $^{14}\text{C}$  measurements from both cores.





## 2.2 Oxygen and carbon stable isotopic measurements

The  $^{18}\text{O}/^{16}\text{O}$  and  $^{13}\text{C}/^{12}\text{C}$  of benthic foraminifera was measured using a Kiel IV Carbonate Device coupled to a Delta XP isotope ratio mass spectrometer at the University of California, Irvine. Isotopic ratios are reported in delta notation, where:

$\delta^{13}\text{C} = (^{13}\text{C}/^{12}\text{C}_{\text{sample}} / ^{13}\text{C}/^{12}\text{C}_{\text{standard}} - 1)$  and  $\delta^{18}\text{O} = (^{18}\text{O}/^{16}\text{O}_{\text{sample}} / ^{18}\text{O}/^{16}\text{O}_{\text{standard}} - 1)$ . Each was multiplied by 1000 to give

5 units of “per mil”. The standard for both measurements is VPDB.

## 2.3 Age model construction for Gulf of California sediment

The age model for LPAZ-21P (between 30,000-to-12,100-kyr Before Physics or “BP,” where BP is 1950) is constrained by 13 microscopic wood fragments calibrated to calendar ages using CALIB7.1 (Stuiver et al., 2017) with the IntCal13

10 atmospheric  $^{14}\text{C}$  dataset (Reimer et al., 2013) (triangles in Figure 3). Five wood measurements from LPAZ-21P did not pass our test for use as an age model constraint (see text below). All LPAZ-21P depths shallower than 63 cm are notably darker, changing from light to very dark brown over a depth interval of  $\approx 2$  cm. The onset of this change is constrained to be younger than  $12,100 \pm 1,100$  years BP ( $12.1 \pm 1.1$ -kyr BP) by a calibrated wood  $^{14}\text{C}$  age (see Appendix). There was a lack of suitable wood in LPAZ-21P in Holocene-aged sediments and our age models for this interval are constrained using *U. peregrina*  $^{14}\text{C}$  15 ages (circles in Figure 3A), corrected for a modern reservoir age of 1240 years based on nearby seawater DIC  $^{14}\text{C}$  age observations at 600 m (Key et al., 2004) and converted to calendar ages using CALIB7.1 (Stuiver et al., 2017). These Holocene  $^{14}\text{C}$  ages are not tied to foraminifera abundance maxima and hence the Holocene calendar ages should be considered preliminary. The youngest calendar age for LPAZ-21P was 5.3-kyr BP, suggesting piston core over-penetration during sediment coring. Samples younger than the LPAZ-21P coretop were obtained from the LPAZ-21PG core, whose age 20 model was constrained identical to the Holocene-aged sediments of LPAZ-21P (see above). The Bayesian age model program BACON (Blaauw and Christen, 2011) was used to estimate the age and model error between the age model constraints.

The ET97-7T age model is constrained in three ways: using  $^{14}\text{C}$  ages of 5 pieces of microscopic wood from 18.9- to 15.3-kyr 25 BP; using *U. peregrina*  $^{14}\text{C}$  ages corrected for reservoir age in Holocene-aged sediment; and by synchronizing the apparently region-wide transition from light to dark-colored sediments (van Geen et al., 2003) to 12.1-kyr based on the wood-constrained age from LPAZ-21P (pink square in Figure 3A). Ages between these constraints were estimated using BACON, as was done for the LPAZ-21P cores.



## 2.4 Wood $^{14}\text{C}$ age test

Terrestrial plant life must have a younger  $^{14}\text{C}$  age / higher  $\Delta^{14}\text{C}$  than contemporaneous foraminifera because of the air-sea difference in  $^{14}\text{C}$  content (e.g., see Figure 1) and we used this inherent  $^{14}\text{C}$  age difference to check for contemporary deposition of the wood and microfossils in Gulf sediments. Fifteen out of 20 microscopic wood fragment  $^{14}\text{C}$  ages passed the test and include one interval that may have been influenced by macrofauna consumption and excretion has a wood  $^{14}\text{C}$  age that is younger than foraminifera (see below).

One wood measurement that spectacularly failed this test came from presumably mid-to-late-Holocene sediment (i.e., <12-kyr BP aged sediments based on the depth below seafloor). However this wood yielded a  $^{14}\text{C}$  age of >25-kyr. We explain this remarkable  $^{14}\text{C}$  age difference as the erosion and deposition of relict wood stored on land before washing to the Gulf during a rain event. The other wood measurements that failed this test gave  $^{14}\text{C}$  ages typically within measurement error or were  $\approx 1000$   $^{14}\text{C}$  years older than foraminifera  $^{14}\text{C}$  age.

In light of this unusual application of calibrated  $^{14}\text{C}$  ages on wood in a marine setting, it is important to understand the potential errors. We assigned all calibrated wood ages a  $\pm 100$  year uncertainty added in quadrature to the measurement and calibration error to account for possible lag in seafloor deposition. A measurement of seawater DIC  $^{14}\text{C}$  age close to our core site and depth (at  $22^\circ\text{N}$ ,  $110^\circ\text{W}$  at 598 m), gives a  $^{14}\text{C}$  age of 1240 years BP. Assuming that DIC at this depth has not yet been seriously impacted by bomb  $^{14}\text{C}$  (Key et al., 2004) this would predict a pre-bomb wood-to-benthic foraminifera  $^{14}\text{C}$  age difference of 1240 years BP. However, the average  $^{14}\text{C}$  age difference between *U. peregrina* and wood used to constrain the age model was  $-2088 \pm 1032$  years, indicating a significant  $^{14}\text{C}$  age difference (and an ‘older’ benthic foraminifera  $^{14}\text{C}$  age). This wood-benthic foraminifera  $^{14}\text{C}$  age difference is far higher than predicted by modern observations, but is consistent with higher atmospheric  $^{14}\text{C}$  content and extreme deglacial  $\Delta^{14}\text{C}$  depletion in intermediate-depth DIC (see Figure 1).

Note that the *asymmetry* of any errors associated with assuming contemporary growth of wood and foraminifera must be considered: if we underestimate the time from wood growth to sediment deposition, the actual calendar age of the sediment would be *younger*; hence foram  $\Delta^{14}\text{C}$  values would be even *lower* than the large depletions shown here (see equation 1 and Results).

## 3 Results

### 3.1 Age model and sedimentation rates

The old coretop age for the LPAZ-21P core (5.3-kyr BP) indicates a poor recovery of the youngest sediments by the piston



core, similar to nearby coring sites on the Pacific margin (van Geen et al., 2003). The LPAZ-21PG gravity core calendar ages range from 7954 to 504 years BP, suggesting that it recovered much of the material missed by the piston core. Both cores give similar sedimentation rates of 16 to 18 cm kyr<sup>-1</sup> over this Holocene interval (see Figure 3A). The nearby trigger core ET97-7T gives a slightly lower sedimentation rate for this time interval (pink in Figure 3), which may result from regional hydrographic differences, different seafloor dynamics, or sediment recovery based on different coring technology. Core recovery equipment may also explain differences in downcore sedimentation rates between the sites (5 cm kyr<sup>-1</sup> versus 19 cm kyr<sup>-1</sup> in ET97-7T during the 13-to-15-kyr BP interval; Figure 3).

The excellent age model controls provided by wood 14C provide us with a powerful (and not always flattering) insight to the sedimentation rates of the Gulf cores. For example, our wood-constrained calendar ages identify two periods of slow sedimentation (or possibly hiatus events) in LPAZ-21P (between 22.7- to 19.5-kyr BP and 12.1- to 9-kyr BP; see grey bars in Figures 3, 4, and 6). The earlier interval is bracketed by wood-constrained calendar ages while the shallower / more recent sedimentation rate slowdown begins approximately at the end of the Younger Dryas or less than ≈12.1-kyr BP.

### 3.2 Foraminifera abundance estimates

The abundance of four benthic and one planktic foraminifera in the LPAZ-21P core is highly variable with the planktic species *G. bulloides* as high as >6000 g<sup>-1</sup> of sediment (Figure 4). The least abundant foraminifera was *P. ariminensis*, which had peak values just over 200 g<sup>-1</sup>. Abundance of *G. bulloides* and all other planktic foraminifera (not shown) in these sediments dropped sharply after 12.1-kyr BP—a loss of planktic foraminifera preservation that is also seen at the nearby California Undercurrent site (red diamond in Figure 2) (Lindsay et al., 2015). The abundance of *P. ariminensis* also drops to zero after 12.9-kyr BP, while *U. peregrina* and *T. bradyi* decline to lower, but persistent values ≈2-kyr later. *Bolivina* spp. are known to persist in low oxygen waters and are the most abundant foraminifera in LPAZ-21P and LPAZ-21PG sediments for the past 7-kyr.

It is important to identify the abundance of sedimentary foraminifera when measuring <sup>14</sup>C because the vertical mixing of sediment by macro- and micro-fauna (bioturbation) can grossly bias the <sup>14</sup>C results (Keigwin and Guilderson, 2009) causing foraminifera <sup>14</sup>C ages to be older on the shallow side of abundance peaks, and vice versa. This effect was recently shown for Juan de Fuca Ridge sediments, where foraminifera <sup>14</sup>C measurements shallower than a large abundance maxima were biased to “old” <sup>14</sup>C ages (Costa et al., 2018). Below we explore the <sup>14</sup>C age and Δ<sup>14</sup>C trends for each benthic foraminifera species.



### 3.3 Comparing benthic foraminifera $^{14}\text{C}$ measurements

We find significant differences in the  $^{14}\text{C}$  age of the four benthic foraminifera species (Figure 5) with a maximum 5775 year offset between *U. peregrina* and *T. bradyi*  $^{14}\text{C}$  age (the former being older). Even though the sample sizes are small (7 to 42), comparing the preferred epifaunal *P. ariminensis* (Keigwin, 2002) to the other species suggests that: (1) *Bolivina* spp.  $^{14}\text{C}$  age is older, (2) *T. bradyi*  $^{14}\text{C}$  age is younger, and that (3) *U. peregrina* gives a  $^{14}\text{C}$  age that is most similar to the epifaunal species (Table 2; left side). Comparing species only at abundance maxima draws from a considerably smaller pool of observations (e.g.,  $n=2$  for the *P. ariminensis* vs. *Bolivina* spp.), but this comparison suggests that—on average—*U. peregrina* ( $n=8$ ) and *T. bradyi* ( $n=4$ ) give similar  $^{14}\text{C}$  ages to epifaunal species, but with a large ( $10\pm 861$  years) to very large ( $35\pm 1125$  years) range of variability. On average, *Bolivina* spp. at abundance maxima ( $n=2$ ) gives an even older  $^{14}\text{C}$  age difference from the preferred epifaunal species (Table 2; right side).

Despite the monospecies  $\Delta^{14}\text{C}$  differences, the glacial-deglacial trends of all four benthic foraminifera  $^{14}\text{C}$  (corrected for decay and shown as  $\Delta^{14}\text{C}$  in Figure 5) from our cores near the mouth of the Gulf of California (the ‘Gulf’ sediment core sites) show a large depletion relative to the atmosphere during the deglaciation—values that are considerably higher during the Holocene and are roughly equal to modern DIC  $\Delta^{14}\text{C}$  measurements at the depth of the cores of  $-173\text{‰}$  (Key et al., 2004). Error bars denote 1 sigma calendar age and  $\Delta^{14}\text{C}$  errors and symbols represent measurements at abundance maxima. Triangles with error bars at bottom of each plot indicate the calendar ages and 1 sigma uncertainties provided by wood dates.

Each monospecies  $\Delta^{14}\text{C}$  record in Figure 5A to D is compared with the nearby benthic foraminifera  $\Delta^{14}\text{C}$  record from the open Pacific margin of Baja California (mostly mixed benthic species on the original age model; see core locations in Figure 2 and Table 1) (Lindsay et al., 2015; Marchitto et al., 2007). Additionally, a series of mixed benthic  $\Delta^{14}\text{C}$  measurements (preliminary work on ET97-7T where species abundance was not quantified) is shown in Figure 5D. All Gulf benthic foraminifera  $\Delta^{14}\text{C}$  measurements are compiled in Figure 5E (black) to illustrate the overall range of values given by the 4 benthic and mixed species measurements relative to the atmospheric (grey; (Reimer et al., 2013)) and the Undercurrent site  $\Delta^{14}\text{C}$  (red). As can be seen by these multiple views of the dataset, all benthic foraminifera  $\Delta^{14}\text{C}$  trends at both Gulf and Undercurrent sites shift to lower values after 20-kyr BP. These depletions relative to atmospheric  $\Delta^{14}\text{C}$  are very large, but even lower  $\Delta^{14}\text{C}$  values are observed for intermediate depth sediment core sites in the eastern equatorial Pacific (Stott et al., 2009).



### 3.4 Influence of macrofaunal consumption and excretion on sediment $^{14}\text{C}$ ages?

In a single interval from 106 to 110 cm of the LPAZ-21P core, which was predicted to be  $\approx 25.5$ -kyr based on interpolation from our Bayesian statistical age model, the wood and benthic and planktic foraminifera  $^{14}\text{C}$  ages were conspicuously younger than expected (Appendix). If these anomalous but self-consistent observations are not simply a result of human error (mislabeling or other sampling problem) they may indicate the presence in this interval of “zoophycos” or the remnants of downward-burrowing macrofauna (as was suggested by (Lougheed et al., 2017)). By consuming and later excreting sedimentary material, these worms are able to move ‘younger’ sedimentary components deeper in the sediment column, though if this is the cause, the self-consistency of our  $^{14}\text{C}$  measurements in this reworked interval (where microfossil and wood  $^{14}\text{C}$  ages suggest an undisturbed sample) is surprising.

10

### 3.5 The stable isotopic composition of oxygen ( $\delta^{18}\text{O}$ ) and carbon ( $\delta^{13}\text{C}$ )

The epifaunal benthic foraminifera (*P. ariminensis*)  $\delta^{18}\text{O}$  and  $\delta^{13}\text{C}$  measurements in Figure 6 uses new and published data from LPAZ-21P (Herguera et al., 2010), but on our wood-constrained age model. As previously reported, intermediate depth  $\delta^{13}\text{C}$  shows little variability between the Last Glacial Maximum (LGM) and Holocene at the depth of this core (624 m; (Herguera et al., 2010)). Benthic foraminifera  $\delta^{18}\text{O}$  is similar to benthic  $\delta^{18}\text{O}$  seen for the nearby Undercurrent core sites (Figure 7 in (Lindsay et al., 2016)) where the  $\delta^{18}\text{O}$  at both sites increase to Holocene values around 13-kyr BP (Figure 6).

15

## 4 Discussion

Based on the work presented here, the trend towards an extreme lowering of intermediate-depth benthic foraminifera  $\Delta^{14}\text{C}$  in the subtropical northeastern Pacific (the California Undercurrent site in Figures 1, 2, and 5) (Lindsay et al., 2015; Marchitto et al., 2007) cannot be explained by species biases, bioturbation, or poor age model controls (Figure 5). This statement is supported by our  $^{14}\text{C}$  measurements of the epifaunal benthic foraminifera *P. ariminensis*—a species known to provide the best record of seawater carbon at the sediment-water interface (Keigwin, 2002)—and several commonly used infaunal benthic foraminifera from sediment cores “upstream” of the canonical record of these extreme  $\Delta^{14}\text{C}$  observations (Figures 1 and 5). Our measurements indicate that even though the potential variability between infaunal and the preferred epifaunal species’  $^{14}\text{C}$  ages is relatively large (several hundred years; Table 2), the average  $^{14}\text{C}$  age difference is  $<100$  years, and the overall trend towards extremely low  $\Delta^{14}\text{C}$  during the deglaciation persists regardless of which species was used.

20

25



#### 4.1 Comparing Gulf and Undercurrent site deglacial records

Our Gulf sediment core observations indicate that the mixed-species  $\Delta^{14}\text{C}$  measurements from the Undercurrent sites shown in Figures 1 and 5 are largely accurate, although the higher values that form the middle of this “W” shaped anomaly (from  $\approx 15$ - to 13-kyr BP) are not obviously reproduced by any of the 4 mono-species benthic foraminifera  $\Delta^{14}\text{C}$ . It is possible that this and other some smaller-scale features of a mixed benthic  $\Delta^{14}\text{C}$  record reflect the bias of a particular species and/or the influence of bioturbation. For example, the benthic foraminifera *T. bradyi* is a possible suspect for biasing mixed benthic  $\Delta^{14}\text{C}$  measurements because it is relatively large, dense, and sometimes has large deviations to younger  $^{14}\text{C}$  ages than the other species (Figure 5). Nevertheless, the overall agreement between the independently derived Undercurrent and Gulf records lend credence to the methods used to construct the age model by (Marchitto et al., 2007) and tested by (Lindsay et al., 2016). We should note that we cannot explain the large offset between the records from 30-to-25-kyr BP, although this comparison only includes one observation from the Undercurrent sites.

The similar  $\Delta^{14}\text{C}$  trends at both Undercurrent and Gulf sites despite sedimentation rate differences and sediment core hiatus lends additional support for the robustness of the  $\Delta^{14}\text{C}$  trends (van Geen et al., 2003; Lindsay et al., 2016) and against events such as the large-scale redeposition of sedimentary components. In principle, the circulation of bottom waters from the Gulf to the Undercurrent sediment core sites could allow for redeposition of benthic foraminifera with much older  $^{14}\text{C}$  ages, but a much larger reworked component (and hence much older benthic foraminifera  $^{14}\text{C}$  ages) would logically be expected at the “upstream” Gulf sites. In fact, sedimentary redeposition should be amplified at the lower sedimentation rate Gulf site, but significantly lower benthic foraminifera  $\Delta^{14}\text{C}$  is not observed for any of the species at the Gulf sites.

These findings allow us to now focus our questions on two potential explanations for the extreme depletions of benthic foraminifera  $\Delta^{14}\text{C}$  observed during the deglaciation: (1) it is a diagenetic signal imparted onto both epifaunal and infaunal foraminifera after burial or (2) it reflects a real change in seawater  $\Delta^{14}\text{C}$  during the deglaciation.

#### 4.2 Can diagenesis explain the low deglacial $\Delta^{14}\text{C}$ ?

Investigating the potential for diagenetic alteration of benthic foraminifera  $\Delta^{14}\text{C}$ , we are not concerned about the newly observed coupling between carbonate dissolution and precipitation (Subhas et al., 2017), which only involves a few monolayers of surface carbonate. Instead, producing the extreme  $\Delta^{14}\text{C}$  lowering observed at Undercurrent and Gulf sites (Figure 5) and other sites around the globe (Bryan et al., 2010; Stott et al., 2009; Thornalley et al., 2011) requires the precipitation of depleted  $^{14}\text{C}$  on or within the foraminifera test is required.



This authigenic calcium carbonate formation and foraminifera  $^{14}\text{C}$  content has been examined in several ways. For example, benthic foraminifera from the eastern equatorial Pacific gives one of the lowest observed deglacial  $\Delta^{14}\text{C}$  values ( $-609\text{‰}$ ), but Scanning Electron Microscope images show no authigenic carbonate on benthic or planktic foraminifera (Stott et al., 2009). Calcium carbonate overgrowth (via the conversion of  $\text{CaCO}_3$  to  $\text{CaSO}_4$  (gypsum)) was observed in Santa Barbara Basin  
5 sediments (Magana et al., 2010), but would not influence the  $^{14}\text{C}$  content of the microfossil. What's more, extreme  $^{14}\text{C}$  depletions of mixed benthic foraminifera from this and other sites were found to be biased by *Pyrgo* spp. (Ezat et al., 2017). Other work suggests *younger-than-expected*  $^{14}\text{C}$  ages from the precipitation of carbonate onto foraminifera tests after core recovery (Skinner et al., 2010). Cook et al., (2011) observed anomalously low foraminifera  $\Delta^{14}\text{C}$ , high  $\delta^{18}\text{O}$ , and low  $\delta^{13}\text{C}$  was consistent with authigenic carbonate precipitation from methane. Similarly, Wycech et al., (2016) compared the  $^{14}\text{C}$  ages  
10 of translucent and opaque mono-specific planktic foraminifera from the same sediment horizons and found the opaque foraminifera (thought to contain authigenic carbonate) had  $^{14}\text{C}$  ages more than 10,000 years older than the translucent tests.

Neither the Gulf nor the Undercurrent site benthic foraminifera measurements display the telltale signs of simultaneous  $\Delta^{14}\text{C}$ ,  $\delta^{18}\text{O}$ , and  $\delta^{13}\text{C}$  anomalies seen by (Cook et al., 2011) (see Figure 6). What's more, the planktic  $\Delta^{14}\text{C}$  from the Undercurrent  
15 site do not show similarly anomalous depletion during the deglaciation (Lindsay et al., 2015), which is expected for post-depositional alteration / authigenic carbonate formation. It is possible that a completely different process of authigenic carbonate formation is occurring in the subtropical eastern Pacific, but we cannot elaborate on what this mechanism might be. It is possible that authigenic carbonates are removed from the foraminiferal test during the 10% acid leaching pre-treatment at KCCAMS (see Methods). This pretreatment was not used in the Wycech et al., (2016) comparisons, but will be  
20 examined in our future studies.

Finally, given the near identical deglacial  $\Delta^{14}\text{C}$  trends at the Undercurrent and Gulf sites despite very different sedimentation rates ( $20\text{--}30\text{ cm kyr}^{-1}$  at the Undercurrent versus  $1\text{--}5\text{ cm kyr}^{-1}$  at the Gulf; Figure 3) it would be surprising if the same depleted  $\Delta^{14}\text{C}$  trends were of diagenetic origin. This is because a faster sedimentation rate will presumably decrease the  
25 potential for authigenic mineralization by decreasing the exposure time of the foraminifera. This reduction in exposure time would apply to both the microfossil's exposure at the sediment-water interface and at sediment depths favorable to authigenic carbonate precipitation. Thus, while the potential influence of authigenic carbonate on the primary foraminifera record is an important area of research that deserves further study, the similarity of the Undercurrent and Gulf records argues against contamination from authigenic carbonate precipitation as the major influence on these benthic foraminifera  $\Delta^{14}\text{C}$   
30 values.



## 5 Conclusions

If the extreme deglacial depletion of benthic foraminifera  $\Delta^{14}\text{C}$  cannot be explained by species or habitat bias, bioturbation, or poor age model control, the remaining explanations appear to be: (1) There was a near synchronous precipitation of  $^{14}\text{C}$ -depleted carbonate on to benthic foraminifera ‘seeds’ in different ocean basins (i.e., the eastern Pacific, southwest Pacific, Indian Ocean, and North Atlantic) or (2) The  $\Delta^{14}\text{C}$  lowering reflects an actual change in seawater DIC  $\Delta^{14}\text{C}$ . The evidence in support of the 2<sup>nd</sup> explanation includes the similarly timed lowering of deep-sea coral  $\Delta^{14}\text{C}$  measurements in both the Southern Ocean and North Atlantic (Adkins et al., 1998; Burke and Robinson, 2012; Chen et al., 2015; Robinson et al., 2005), which are often on rocky seamounts and should not be influenced by the same diagenetic processes. If the  $\Delta^{14}\text{C}$  change was real, a leading candidate among the potential explanations is the deep-sea sequestration and flushing of carbon through the intermediate depth ocean. However, matching the observed  $\Delta^{14}\text{C}$  depletions appears to require unrealistic changes in ocean chemistry (e.g., lower surface ocean alkalinity) and ocean dynamics (i.e., mixing) (Hain et al., 2011).

An alternative explanation involves the addition of  $^{14}\text{C}$ -depleted carbon via mid-ocean ridge (MOR) volcanism (Ronge et al., 2016), which is indirectly supported by evidence for increased MOR activity (Lund, 2013; Middleton et al., 2016; Tolstoy, 2015, 2015). The locations and depths of the extreme benthic foraminifera  $\Delta^{14}\text{C}$  lowering are also suggestive of a MOR influence, given their proximity to the East Pacific Rise / Gulf of California (Marchitto et al., 2007; Ronge et al., 2016; Stott et al., 2009; this study), the Red Sea (Bryan et al., 2010), and Mid-Atlantic Ridge (Thornalley et al., 2011). However, this hypothesis of enhanced carbon flux from seafloor volcanism must also explain the many intermediate-depth sites that do not show anomalous deglacial  $\Delta^{14}\text{C}$  depletions (e.g., (Broecker & Clark, 2010; Cléroux et al., 2011; De Pol-Holz et al., 2010)). Furthermore, this proposed carbon addition must have been associated with an alkalinity addition, without which the increased seawater  $\text{CO}_2$  concentrations and therefore lower seawater pH would have caused a global-scale carbonate dissolution event (Stott and Timmermann, 2011).

In summary, our work strongly suggests that at least for the Gulf of California and adjacent Pacific sites, the foraminifera  $\Delta^{14}\text{C}$  proxy records real  $^{14}\text{C}$  changes in deglacial intermediate depth seawater DIC, but the question of what caused those changes remains open. Careful examination to confirm or disprove the fidelity of the benthic foraminifera  $\Delta^{14}\text{C}$  on a case by case basis will be a critical part of building a reliable body of data to identify the controls on glacial-interglacial marine carbon cycling.

## 30 Acknowledgments

C. Bertrand, A. Hangsterfer (SIO Core Repository), H. Martinez, N. Shammass, M. Ayad, M. Rudresh, A. De la Rosa, J. Troncoso, J. DeLine, J. Sanchez, C. Manlapid, and M. Chan.





## References

- Adkins, J. F., Cheng, H., Boyle, E. A., Druffel, E. R. M. and Edwards, L. R.: Deep-Sea Coral Evidence for Rapid Change in Ventilation of the Deep North Atlantic 15,400 Years Ago, *Science*, 280, 1998.
- Ahn, J. and Brook, E. J.: Siple Dome ice reveals two modes of millennial CO<sub>2</sub> change during the last ice age, *Nat. Commun.*, 5(1), doi:10.1038/ncomms4723, 2014.
- Blaauw, M. and Christen, J. A.: Flexible paleoclimate age-depth models using an autoregressive gamma process., *Bayesian Anal.*, 6, 457–474, 2011.
- Broecker, W. S.: Glacial to interglacial changes in ocean chemistry, *Prog. Oceanogr.*, 11, 1982.
- Broecker, W. S. and Barker, S.: A 190‰ drop in atmosphere's  $\Delta^{14}\text{C}$  during the “Mystery Interval” (17.5 to 14.5 kyr), *Earth Planet. Sci. Lett.*, 256(1–2), 90–99, doi:10.1016/j.epsl.2007.01.015, 2007.
- Broecker, W. S. and Clark, E.: Search for a glacial-age  $^{14}\text{C}$ -depleted ocean reservoir, *Geophys. Res. Lett.*, 37(13), 1–6, doi:10.1029/2010GL043969, 2010.
- Broecker, W. S., Klas, M., Ragano-Beavan, N., Mathieu, G. and Mix, A.: Accelerator mass spectrometry radiocarbon measurements on marine carbonate samples from deep sea cores and sediment traps, *Radiocarbon*, 30(3), 35, 1988.
- Bryan, S. P., Marchitto, T. M. and Lehman, S. J.: The release of  $^{14}\text{C}$ -depleted carbon from the deep ocean during the last deglaciation: Evidence from the Arabian Sea, *Earth Planet. Sci. Lett.*, 298(1–2), 244–254, doi:10.1016/j.epsl.2010.08.025, 2010.
- Burke, A. and Robinson, L.: The Southern Ocean's Role in Carbon Exchange During the Last Deglaciation, *Science*, 335(6068), 557–561, doi:10.1126/science.1215110, 2012.
- Chen, T., Robinson, L. F., Burke, A., Southon, J., Spooner, P., Morris, P. J. and Ng, H. C.: Synchronous centennial abrupt events in the ocean and atmosphere during the last deglaciation, *Science*, 349(6255), 1537–1541, doi:10.1126/science.aac6159, 2015.
- Clérout, C., deMenocal, P. and Guilderson, T.: Deglacial radiocarbon history of tropical Atlantic thermocline waters: absence of CO<sub>2</sub> reservoir purging signal, *Quat. Sci. Rev.*, 30(15–16), 1875–1882, doi:10.1016/j.quascirev.2011.04.015, 2011.
- Cook, M. S., Keigwin, L. D., Birgel, D. and Hinrichs, K.-U.: Repeated pulses of vertical methane flux recorded in glacial sediments from the southeast Bering Sea, *Paleoceanography*, 26(2), n/a-n/a, doi:10.1029/2010PA001993, 2011.
- Costa, K. M., McManus, J. F. and Anderson, R. F.: Radiocarbon and Stable Isotope Evidence for Changes in Sediment Mixing in the North Pacific over the Past 30 kyr, *Radiocarbon*, 60(01), 113–135, doi:10.1017/RDC.2017.91, 2018.
- De Pol-Holz, R., Keigwin, L., Southon, J., Hebbeln, D. and Mohtadi, M.: No signature of abyssal carbon in intermediate waters off Chile during deglaciation, *Nat. Geosci.*, 3(3), 192–195, doi:10.1038/ngeo745, 2010.



- Ezat, M. M., Rasmussen, T. L., Thornalley, D. J. R., Olsen, J., Skinner, L. C., Hönisch, B. and Groeneveld, J.: Ventilation history of Nordic Seas overflows during the last (de)glacial period revealed by species-specific benthic foraminiferal  $^{14}\text{C}$  dates, *Paleoceanography*, 32(2), 172–181, doi:10.1002/2016PA003053, 2017.
- Field, D. B.: Variability in vertical distributions of planktonic foraminifera in the California Current: Relationships to vertical ocean structure, *Paleoceanography*, 19(2), n/a-n/a, doi:10.1029/2003PA000970, 2004.
- Galbraith, E. D., Jaccard, S. L., Pedersen, T. F., Sigman, D. M., Haug, G. H., Cook, M., Southon, J. R. and Francois, R.: Carbon dioxide release from the North Pacific abyss during the last deglaciation, *Nature*, 449(7164), 890–U9, doi:10.1038/nature06227, 2007.
- van Geen, A., Zheng, Y., Bernhard, J. M., Cannariato, K. G., Carriquiry, J., Dean, W. E., Eakins, B. W., Ortiz, J. D. and Pike, J.: On the preservation of laminated sediments along the western margin of North America, *Paleoceanography*, 18(4), doi:10.1029/2003pa000911, 2003.
- Gómez-Valdivia, F., Parés-Sierra, A. and Flores-Morales, A. L.: The Mexican Coastal Current: A subsurface seasonal bridge that connects the tropical and subtropical Northeastern Pacific, *Cont. Shelf Res.*, 110, 100–107, doi:10.1016/j.csr.2015.10.010, 2015.
- Hain, M. P., Sigman, D. M. and Haug, G. H.: Shortcomings of the isolated abyssal reservoir model for deglacial radiocarbon changes in the mid-depth Indo-Pacific Ocean, *Geophys. Res. Lett.*, 38, doi:10.1029/2010gl046158, 2011.
- Herguera, J. C., Herbert, T., Kashgarian, M. and Charles, C.: Intermediate and deep water mass distribution in the Pacific during the Last Glacial Maximum inferred from oxygen and carbon stable isotopes, *Quat. Sci. Rev.*, 29(9–10), 1228–1245, doi:10.1016/j.quascirev.2010.02.009, 2010.
- Jaccard, S. L. and Galbraith, E. D.: Large climate-driven changes of oceanic oxygen concentrations during the last deglaciation, *Nat. Geosci.*, 5(2), 151–156, doi:10.1038/ngeo1352, 2011.
- Jaccard, S. L., Galbraith, E. D., Martínez-García, A. and Anderson, R. F.: Covariation of deep Southern Ocean oxygenation and atmospheric  $\text{CO}_2$  through the last ice age, *Nature*, 530(7589), 207–210, doi:10.1038/nature16514, 2016.
- Keeling, C. D.: The concentration and isotopic abundances of carbon dioxide in the atmosphere, *Tellus*, 12(2), 1960.
- Keigwin, L. D.: Late Pleistocene-Holocene paleoceanography and ventilation of the Gulf of California, *J. Oceanogr.*, 58(2), 421–432, 2002.
- Keigwin, L. D. and Guilderson, T. P.: Bioturbation artifacts in zero-age sediments, *Paleoceanography*, 24(4), doi:10.1029/2008PA001727, 2009.
- Keigwin, L. D. and Lehman, S. J.: Radiocarbon evidence for a possible abyssal front near 3.1 km in the glacial equatorial Pacific Ocean, *Earth Planet. Sci. Lett.*, 425, 93–104, doi:10.1016/j.epsl.2015.05.025, 2015.
- Key, R. M., Kozyr, A., Sabine, C. L., Lee, K., Wanninkhof, R., Bullister, J. L., Feely, R. A., Millero, F. J., Mordy, C. and Peng, T. H.: A global ocean carbon climatology: Results from Global Data Analysis Project (GLODAP), *Glob. Biogeochem. Cycles*, 18(4), doi:10.1029/2004gb002247, 2004.



- Lindsay, C. M., Lehman, S. J., Marchitto, T. M. and Ortiz, J. D.: The surface expression of radiocarbon anomalies near Baja California during deglaciation, *Earth Planet. Sci. Lett.*, 422, 67–74, doi:10.1016/j.epsl.2015.04.012, 2015.
- Lindsay, C. M., Lehman, S. J., Marchitto, T. M., Carriquiry, J. D. and Ortiz, J. D.: New constraints on deglacial marine radiocarbon anomalies from a depth transect near Baja California, *Paleoceanography*, 31(8), 1103–1116, doi:10.1002/2015PA002878, 2016.
- Lougheed, B. C., Metcalfe, B., Ninnemann, U. S. and Wacker, L.: Moving beyond the age-depth model paradigm in deep sea palaeoclimate archives: dual radiocarbon and stable isotope analysis on single foraminifera, *Clim. Past Discuss.*, 1–16, doi:10.5194/cp-2017-119, 2017.
- Lund, D. C.: Deep Pacific ventilation ages during the last deglaciation: Evaluating the influence of diffusive mixing and source region reservoir age, *Earth Planet. Sci. Lett.*, 381, 52–62, doi:10.1016/j.epsl.2013.08.032, 2013.
- MacFarling Meure, C., Etheridge, D., Trudinger, C., Steele, P., Langenfelds, R., van Ommen, T., Smith, A. and Elkins, J.: Law Dome CO<sub>2</sub>, CH<sub>4</sub> and N<sub>2</sub>O ice core records extended to 2000 years BP, *Geophys. Res. Lett.*, 33(14), doi:10.1029/2006GL026152, 2006.
- Magana, A. L., Southon, J. R., Kennett, J. P., Roark, E. B., Sarnthein, M. and Stott, L. D.: Resolving the cause of large differences between deglacial benthic foraminifera radiocarbon measurements in Santa Barbara Basin, *Paleoceanography*, 25(4), doi:10.1029/2010PA002011, 2010.
- Marchitto, T. M., Lehman, S. J., Ortiz, J. D., Fluckiger, J. and van Geen, A.: Marine Radiocarbon Evidence for the Mechanism of Deglacial Atmospheric CO<sub>2</sub> Rise, *Science*, 316, 1456–1459, 2007.
- Marcott, S. A. and Shakun, J. D.: A record of ice sheet demise, *Science*, 358(6364), 721–722, doi:10.1126/science.aaq1179, 2017.
- Middleton, J. L., Langmuir, C. H., Mukhopadhyay, S., McManus, J. F. and Mitrovica, J. X.: Hydrothermal iron flux variability following rapid sea level changes, *Geophys. Res. Lett.*, 43(8), 3848–3856, doi:10.1002/2016GL068408, 2016.
- Monnin, E.: Atmospheric CO<sub>2</sub> Concentrations over the Last Glacial Termination, *Science*, 291(5501), 112–114, doi:10.1126/science.291.5501.112, 2001.
- Petit, J. R., Jouzel, J., Raynaud, D., Barkov, N. I., Barnola, J. M., Basile, I., Bender, M., Chappellaz, J., Davis, M., Delaygue, G., Delmotte, M., Kotlyakov, V. M., Legrand, M., Lipenkov, V. Y., Lorius, C., Pepin, L., Ritz, C., Saltzman, E. and Stievenard, M.: Climate and atmospheric history of the past 420,000 years from the Vostok ice core, Antarctica, *Nature*, 399(6735), 429–436, 1999.
- Reimer, P., Bard, E., Bayliss, A., Beck, J., Blackwell, P., Bronk, R., Buck, C., Cheng, H., Edwards, R., Friedrich, M., Grootes, P., Guilderson, T., Hafliðason, H., Hajdas, I., Hatte, C., Heaton, T., Hoffmann, D., Hogg, A., Hughen, K., Kaiser, K., Kromer, B., Manning, S., Niu, M., Reimer, R., Richards, D., Scott, E., Southon, J., Staff, R., Turney, C. and van der Plicht, J.: IntCal13 and Marine13 radiocarbon age calibration curves 0–50,000 years cal BP., *Radiocarbon*, 55(4), 1869–1887, 2013.



- Robinson, L. F., Adkins, J. F., Keigwin, L. D., Southon, J., Fernandez, D. P., Wang, S.-L. and Scheirer, D. S.: Radiocarbon Variability in the Western North Atlantic During the Last Deglaciation, *Science*, 310, 1469–1473, 2005.
- Ronge, T. A., Tiedemann, R., Lamy, F., Köhler, P., Alloway, B. V., De Pol-Holz, R., Pahnke, K., Southon, J. and Wacker, L.: Radiocarbon constraints on the extent and evolution of the South Pacific glacial carbon pool, *Nat. Commun.*, 7, 11487, doi:10.1038/ncomms11487, 2016.
- 5 Rose, K. A., Sikes, E. L., Guilderson, T. P., Shane, P., Hill, T. M., Zahn, R. and Spero, H. J.: Upper-ocean-to-atmosphere radiocarbon offsets imply fast deglacial carbon dioxide release, *Nature*, 466(7310), 1093–1097, doi:10.1038/nature09288, 2010.
- Santos, G. M., Moore, R. B., Southon, J. R., Griffin, S., Hinger, E. and Zhang, D.: AMS 14C sample preparation at the KCCAMS/UCI Facility: status report and performance of small samples, *Radiocarbon*, 49(2), 255–270, 2007.
- 10 Sikes, E. L., Samson, C. R., Guilderson, T. P. and Howard, W. R.: Old radiocarbon ages in the southwest Pacific Ocean during the last glacial period and deglaciation, *Nature*, 405, 6, 2000.
- Skinner, L. C., Fallon, S., Waelbroeck, C., Michel, E. and Barker, S.: Ventilation of the Deep Southern Ocean and Deglacial CO<sub>2</sub> Rise, *Science*, 328(5982), 1147–1151, 2010.
- 15 Southon, J., Santos, G., Druffel-Rodriguez, K., Druffel, E., Trumbore, S., Xu, X., Griffin, S., Ali, S. and Mazon, M.: The Keck Carbon Cycle AMS laboratory, University of California, Irvine: initial operation and a background surprise, *Radiocarbon* [online] Available from: <https://escholarship.org/uc/item/0xw7c8b3.pdf> (Accessed 10 June 2016), 2004.
- Stott, L. and Timmermann, A.: Hypothesized Link Between Glacial/Interglacial Atmospheric CO<sub>2</sub> Cycles and Storage/Release of CO<sub>2</sub>-Rich Fluids From Deep-Sea Sediments, in *Geophysical Monograph Series*, vol. 193, edited by H. Rashid, L. Polyak, and E. Mosley-Thompson, pp. 123–138, American Geophysical Union, Washington, D. C., 2011.
- 20 Stott, L., Southon, J., Timmermann, A. and Koutavas, A.: Radiocarbon age anomaly at intermediate water depth in the Pacific Ocean during the last deglaciation, *Paleoceanography*, 24(2), doi:10.1029/2008PA001690, 2009.
- Stuiver, M. and Polach, H. A.: Discussion; reporting of C-14 data., *Radiocarbon*, 19(3), 355–363, 1977.
- Stuiver, M., Reimer, P. and Reimer, R.: CALIB 7.1. [online] Available from: <http://calib.org> (Accessed 2 January 2017), 2017.
- 25 Subhas, A. V., Adkins, J. F., Rollins, N. E., Naviaux, J., Erez, J. and Berelson, W. M.: Catalysis and chemical mechanisms of calcite dissolution in seawater, *Proc. Natl. Acad. Sci.*, 114(31), 8175–8180, doi:10.1073/pnas.1703604114, 2017.
- Thornalley, D. J. R., Barker, S., Broecker, W. S., Elderfield, H. and McCave, I. N.: The Deglacial Evolution of North Atlantic Deep Convection, *Science*, 331(6014), 202–205, doi:10.1126/science.1196812, 2011.
- 30 Tolstoy, M.: Mid-ocean ridge eruptions as a climate valve, *Geophys. Res. Lett.*, 42(5), 1346–1351, doi:10.1002/2014GL063015, 2015.
- Wycech, J., Kelly, D. C. and Marcott, S.: Effects of seafloor diagenesis on planktic foraminiferal radiocarbon ages, *Geology*, 44(7), 551–554, doi:10.1130/G37864.1, 2016.

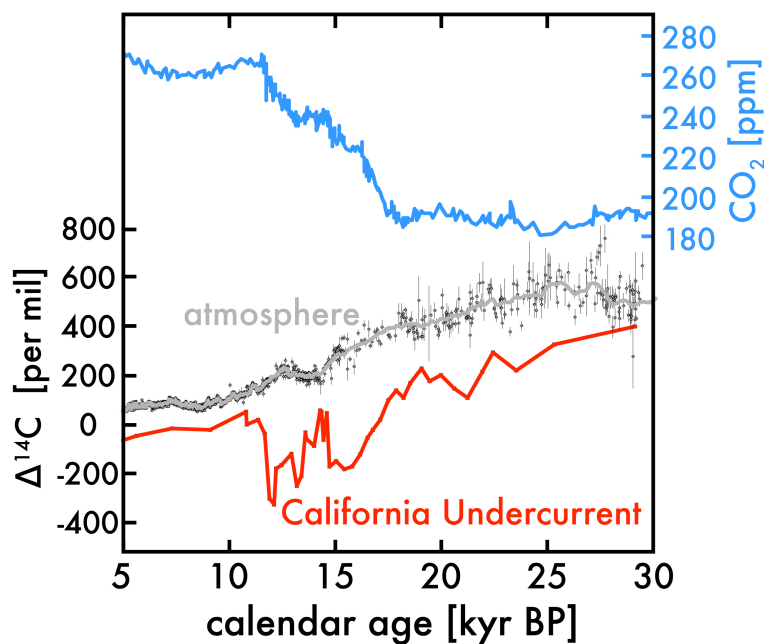


Figure 1. Atmospheric carbon dioxide ( $\text{CO}_2$ ) concentrations (blue; top) (Ahn and Brook, 2014; MacFarling Meure et al., 2006; Marcott and Shakun, 2017; Monnin, 2001), atmospheric  $\Delta^{14}\text{C}$  (gray; middle) (Reimer et al., 2013), and benthic foraminifera  $\Delta^{14}\text{C}$  from sediment bathed in California Undercurrent water (red; see Table 1 and maps in Figure 2) (Lindsay et al., 2015; Marchitto et al., 2007). These observations are shown from 30-to-5-kyr BP (BP = before 1950).

5

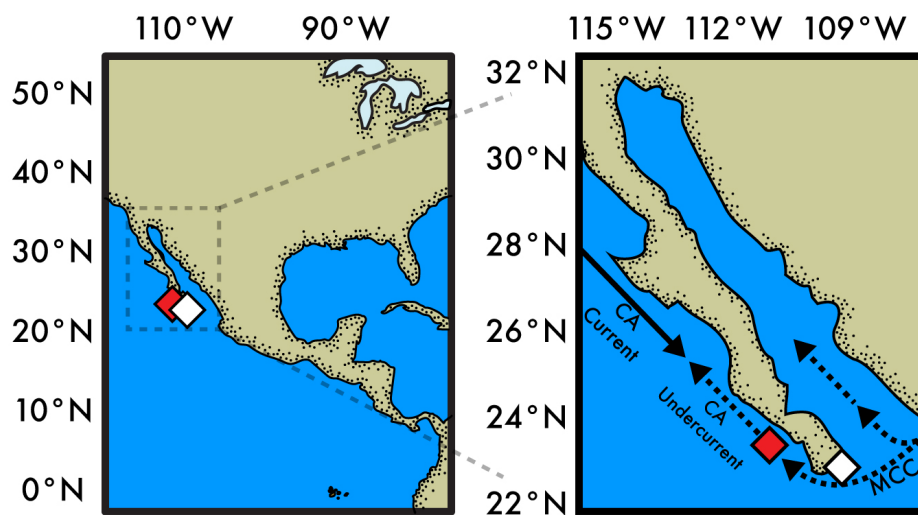


Figure 2. Maps of sediment core sites (diamonds; see Table 1) and ocean circulation (arrows: solid = surface; dashed = near seafloor). The foraminifera radiocarbon measurements in Figure 1 are from core sites at the red diamond (Marchitto et al., 2007; Lindsay et al., 2016). See Table 1 for details on site locations. Note that the subsurface Mexican Coastal Current (MCC) flows between 200 to  $\approx 700$  m and feeds subsurface water into both the Gulf of California and California Undercurrent (Gómez-Valdivia et al., 2015)—waters that bathe both core sites.

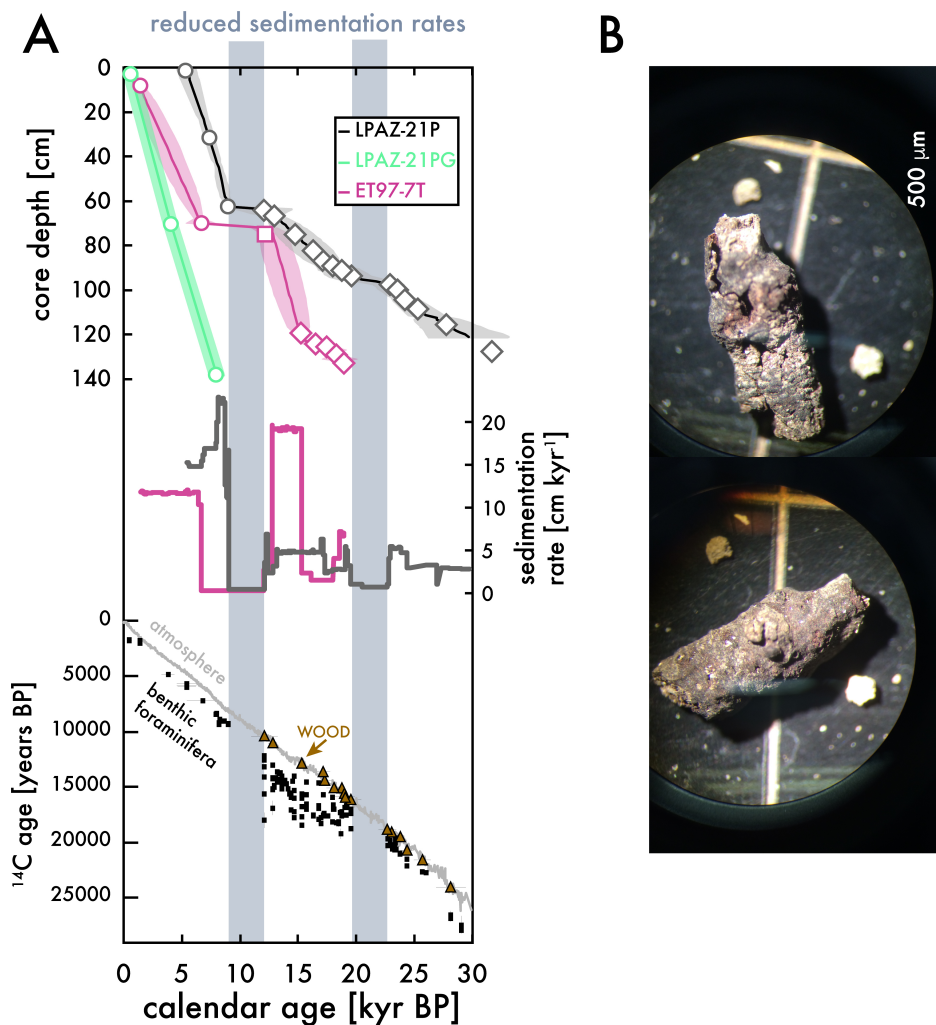


Figure 3. (A) Sediment core depth (top), sedimentation rate (middle), and the <sup>14</sup>C age of atmospheric CO<sub>2</sub>, benthic foraminifera, and wood (bottom) versus calendar age (thousands of years BP or kyr BP) for sites LPAZ-21P, LPAZ-21PG, and ET97-7T (see Figure 1 and Table 1 for locations). (B) Examples of wood found within sediment core LPAZ-21P.

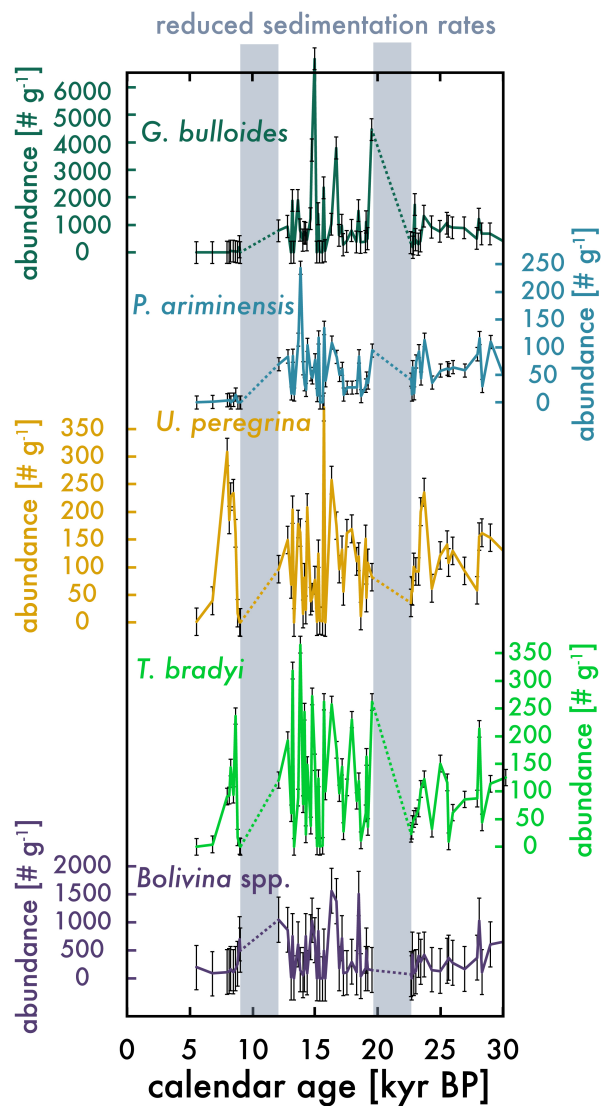


Figure 4. Foraminifera abundance at site LPAZ-21P for planktic (*G. bulloides*) and benthic species (all others).



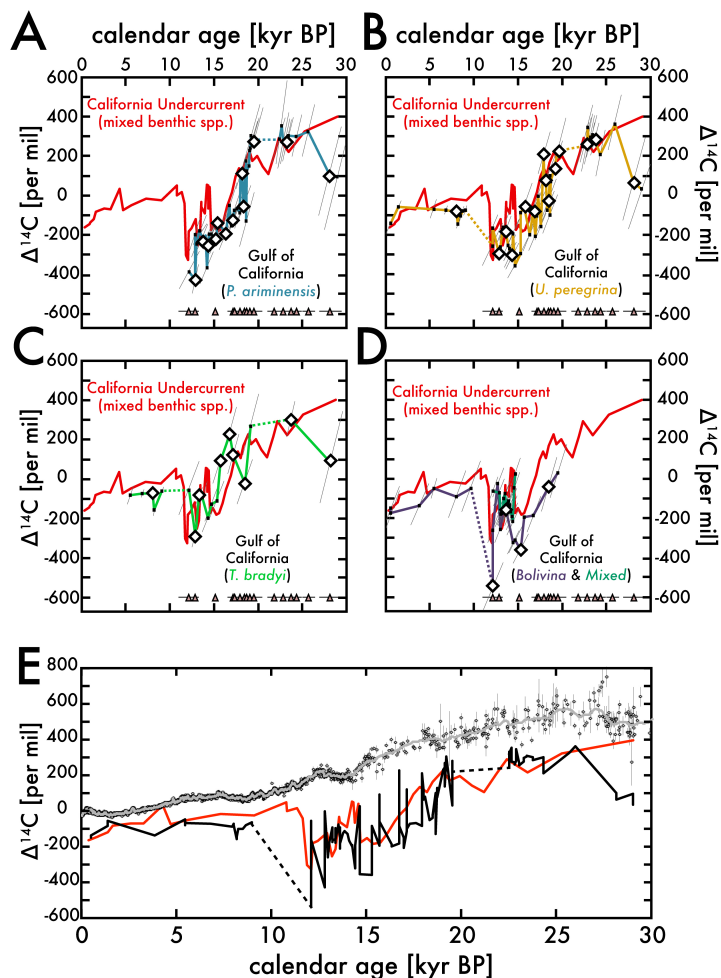


Figure 5. The  $\Delta^{14}\text{C}$  isotopic composition (corrected for decay as  $\Delta^{14}\text{C}$ ) for Gulf of California benthic foraminifera mono-species (A-D) and mixed species (D) are compared with mono- and mixed-species benthic foraminifera  $\Delta^{14}\text{C}$  measurements from the California Undercurrent sediment core site (red) (Lindsay et al., 2015; Marchitto et al., 2007) over the past 35,000 years BP. See core locations in Figure 2. Canted error bars take into account measurement and age model errors (Stuiver et al., 2017). The  $\Delta^{14}\text{C}$  of all Gulf benthic foraminifera is shown in (E) alongside atmospheric  $\Delta^{14}\text{C}$  (grey) (Reimer et al., 2013) and California Undercurrent site  $\Delta^{14}\text{C}$  (red). Modern  $\Delta^{14}\text{C}$  near the depth of the Gulf and Pacific sites (red and black in E) is about -173‰ (Key et al., 2004).

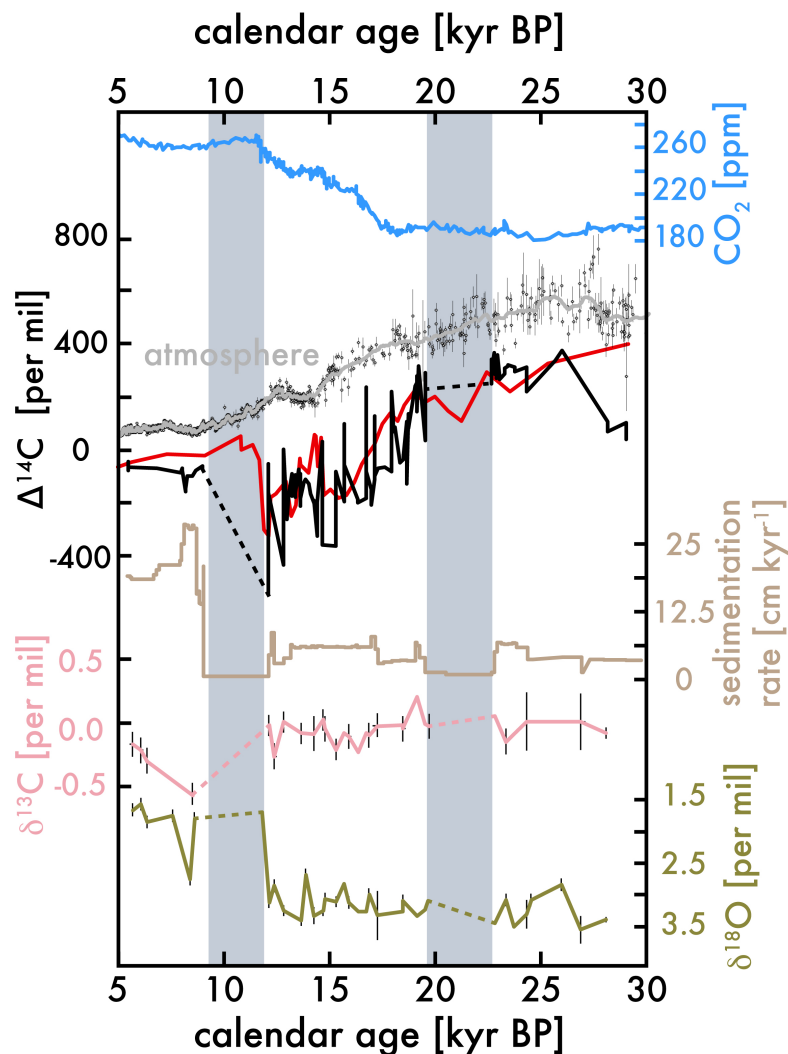


Figure 6. From top to bottom: atmospheric carbon dioxide ( $\text{CO}_2$ ) (blue; same as Figure 1), atmospheric  $\text{CO}_2$   $\Delta^{14}\text{C}$  (grey; same as Figure 1), mixed and mono-species benthic foraminifera  $\Delta^{14}\text{C}$  from the California Undercurrent site (red) (Lindsay et al., 2015; Marchitto et al., 2007), all mono-species benthic foraminifera  $\Delta^{14}\text{C}$  from near the mouth of the Gulf of California (black; this study), sedimentation rate of LPAZ-21P (see Figure 3), benthic foraminifera *P. ariminensis*  $\delta^{13}\text{C}$  (pink) and  $\delta^{18}\text{O}$  (green) from this study and Herguera et al., (2010).

5



**Table 1.** Latitude, longitude, depth below modern sea surface, and modern dissolved inorganic carbon (DIC)  $\Delta^{14}\text{C}$  (26) at the sediment-seawater interface for sediment cores discussed in this study.

| Table 1              | latitude<br>[°N] | longitude [°W] | depth [m] | modern DIC<br>$\Delta^{14}\text{C}$ [‰] at<br>this depth |
|----------------------|------------------|----------------|-----------|--|
| LPAZ-21P / LPAZ-21PG | 22.9             | 109.5          | 624       | -148   |
| ET97-7T              | 22.9             | 109.5          | 640       | -148   |
| MV99-MC19/GC31/PC08  | 23.5             | 111.6          | 705       | -148   |

**Table 2.** Comparison between benthic foraminifera  $^{14}\text{C}$  ages for all measurements (“ALL”) and only at abundance maxima (see Figure 4).

| The difference between <i>P. ariminensis</i> - <i>U. peregrina</i> [ <sup>14</sup> C years] |                  | The difference between <i>P. ariminensis</i> - <i>T. bradyi</i> [ <sup>14</sup> C years] |                  | The difference between <i>P. ariminensis</i> - <i>Bolivina</i> spp [ <sup>14</sup> C years] |                  |       |
|---|------------------|--|------------------|---|------------------|-------|
| ALL   | abundance maxima | ALL  | abundance maxima | ALL   | abundance maxima |       |
| AVERAGE   | -104             | 10   | 826              | 35  | -857             | -1407 |
| STDEV   | 759              | 861  | 1484             | 1125  | 939              | 597   |
| n   | 42               | 8  | 7                | 4   | 11               | 2     |